Limitations in Existing Methods for Analysing MSE Walls Reinforced with Steel Strips

Lalinda Weerasekara, Ph.D., P.Eng.
Senior Geotechnical Engineer, WSP Canada Inc., Nanaimo, BC.

ABSTRACT The current practice for designing mechanically stabilized earth (MSE) structures involves empirical methods to estimate the maximum reinforcement loads using different variants of tributary area method (e.g., AASHTO Simplified, Coherent Gravity and Simplified Stiffness methods) which were validated only for working stress conditions. Since soil-reinforcement interaction is not explicitly accounted in these methods, there are key limitations in attempting to estimating the ultimate state especially in walls with inextensible reinforcements. This paper compares above design methods against the Soil Reinforcement Interaction (SRI) method, an analytical solution that considers the complex soil-reinforcement interaction occurring in MSE walls. Several critical shortcomings of the current state practice can be overcome using this method, including the ability to (i) estimate the ultimate state by considering more realistic failure modes, (ii) estimate the load transmitted to the facing connection, (iii) estimate the tensile force distribution along the reinforcement (iv) quantify the toe resistance (v) analyse walls with non-uniform reinforcement lengths and configurations (vi) design for vertical and horizontal obstructions and (vii) explain different behavioural characteristics. Where applicable, actual instrumented walls are utilized to demonstrate these benefits. The paper focuses mainly on walls reinforced with inextensible reinforcements where above shortcomings have the greatest impact.

Introduction

This paper attempts to highlight some of the key limitations of existing design methods available for estimating the internal stability of Mechanically Stabilized Earth (MSE) walls and how those can be overcome using the Soil Reinforcement Interaction (SRI) method. The paper focuses mainly on walls reinforced with inextensible reinforcements such as steel strips, although certain comments are also applicable to MSE walls with extensible reinforcements. For comparison purposes, Coherent Gravity (Schlosser 1978), AASHTO Simplified (AASHTO 2020) and Simplified Stiffness (Allen and Bathurst 2015) methods are considered in this paper. First two methods are recommended in the American Association of State Highway and Transportation Officials (AASHTO) and Canadian Highway Bridge Design Code (Canadian Standards Association 2019). for the design of MSE walls with inextensible reinforcements. In these methods, the maximum reinforcement forces (P_{max}) in the most general form, is calculated based on the tributary area concept as follows:

[1] $$P_{max} = K\,\sigma'_v\,S_v S_h$$

σ'_v is the vertical effective stress at reinforcement level, S_v and S_h are the vertical and horizontal spacings between reinforcements and K is an empirical lateral earth pressure coefficient which is back calculated from instrumented walls. Consequently, different K values and distributions with depth are considered to demonstrate the differences in reinforcement stiffnesses and soil-reinforcement interactions. Using P_{max} calculated for each reinforcement layer, the following three failure mechanisms are evaluated for each reinforcement layer: (a) tensile rupture of the reinforcement, (b) pullout and (c) connection failure.

Soil Reinforcement Interaction (SRI) Method

A brief description of the SRI method is given below and further details can be found in Weerasekara et al. (2017). The SRI method is a combination of the following three sub-models:

1. SRI Friction model: A model to account for the frictional forces at the soil-reinforcement interface.
2. SRI Local model: An analytical solution to model the soil-reinforcement interaction in each reinforcement; and
3. SRI Global model: An approach to account for the equilibrium and interaction of multiple reinforcements in the reinforced soil mass.

SRI Friction Model

The friction per unit length (T) at the soil-reinforcement interface is expressed using a bi-linear model (Fig. 1), where the peak frictional resistance (T_1) is expressed in the following form.

[2] $$T_1 = \frac{2bH\gamma \tan\varphi'_g}{1-[2(1+\nu)/((1-2\nu)(1+2K_0))]\tan\varphi'_g \tan\psi_{max}}$$

where b is the width of the reinforcement, H is the burial depth, γ is the unit weight of the soil overburden, φ'_g is the soil-reinforcement interface friction angle, υ is the Poisson's ratio of soil, K_0 is the lateral earth pressure coefficient at-rest and ψ_{max} is the peak angle of dilation. As the magnitude of soil dilation depends on the mean effective stress, the classical stress-dilatancy framework proposed by Bolton (1986) can be used to express ψ_{max} in the following form:

$$\Psi_{max} = 6.25(I_D(Q - ln\sigma') - R) \quad [3]$$

$$\Psi_{max} = 6.25(I_D(Q - ln\sigma') - R)$$

where σ' is the mean effective stress and I_D is the relative density of the soil which can be obtained from conventional testing or approximately estimated based on the degree of compaction or measured soil unit weight. Parameters Q and R are the only empirical parameters in the model which generally depend on the soil type. The frictional resistance attributed to soil dilation is expected to decrease gradually and becomes negligible at a displacement of ($\overline{u_2}$). Above is an important consideration for extensible reinforcements because different sections of the reinforcement will experience different magnitudes of friction due to the progressive development of friction along the reinforcement. At a displacement of ($\overline{u_2}$), the interface friction per unit length (T_2) is given by the following:

$$T_2 = 2bH\gamma \tan \varphi'_g \quad [4]$$

The value of $\overline{u_2}$ is typically obtained from experimental observations. For a typical MSE wall, the results are relatively insensitive to the value selected for $\overline{u_2}$. Guidelines related to the selection of input parameters is given in Weerasekara et al. (2017).

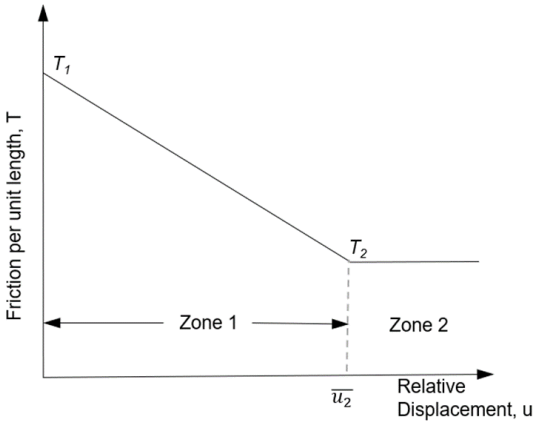

Fig. 1. Schematic representation of SRI Friction model

$$T_1 = \frac{2bH\gamma \tan \varphi'_g}{1-[2(1+v)/((1-2v)(1+2K_0))]\tan \varphi'_g \tan \psi_{max}}$$

SRI Local Model

Using the interface frictional model and reinforcement stiffness, the following governing equations of the SRI Local model can be obtained by considering the force equilibrium at an element level.

$$u = \left(\frac{\kappa}{\lambda}\right)\left(1 - \cos\sqrt{\lambda}l\right) \quad [5]$$

$$\varepsilon = \left(\frac{\kappa}{\sqrt{\lambda}}\right)\left(\sin\sqrt{\lambda}l\right) \quad [6]$$

where,

$\lambda = \frac{(T_1 - T_2)}{J_r \overline{u_2}}$ and $\kappa = \frac{T_1}{J_r}$ with $\sqrt{\lambda}l < \frac{\pi}{2}$

l is the mobilized friction length along the reinforcement due to the displacement occurring at the failure plane of the MSE wall. In a pullout test, u is displacement at the pulling end which is equivalent to one-half of the separation of the stable and unstable soil masses along the failure plane of the MSE wall. J_r is the axial stiffness of the reinforcement which is equal to the reinforcement modulus multiplied by the cross-sectional area. In terms of steel strip reinforcements, this represents the Young's modulus times the total cross-sectional area of steel strips encountered within a unit width.

If the displacement is known, the mobilized frictional length along the reinforcement (l) can be obtained by rearranging Eq. (5) as follows:

$$l = \left(\frac{1}{\sqrt{\lambda}}\right)\cos^{-1}\left(1 - \frac{u\lambda}{\kappa}\right)$$

$$l = \left(\frac{1}{\sqrt{\lambda}}\right)\cos^{-1}\left(1 - \frac{u\lambda}{\kappa}\right) \quad [7]$$

Knowing the strain, tensile force in the reinforcement at any given location can be obtained as follows:

$$P = J_r \times \varepsilon \quad [8]$$

Above analytical approach provides a framework to relate the displacement, strain, force and mobilized frictional length along the reinforcement. If any single parameter is known, the remaining three parameters can be estimated.

In this formulation, it is important to highlight the difference between P and T. Note that T acts on the reinforcement as an external frictional force and independent of the reinforcement stiffness, while P is the force developed in the reinforcement due to this

external force and depends on the reinforcement stiffness. This difference is often overlooked and has led to several confusions.

SRI Global Model

The SRI Global model provides a framework to assess the stability of the entire reinforced soil mass, such that the total resistance provided by the soil reinforcements are equated to the total driving forces from earth pressures, surcharge and other loads that contributes to the instability. The lateral earth pressure will continue to decrease from at-rest condition and reach the active state if the displacement is large enough. While this occurs, the resistance from reinforcements will increase as the soil mass displaces. For this computation, the moments are calculated about the base of the wall since the mobilized resistance at this location (R_T) is not typically known. The equilibrium is reached when the total driving moment is equal to the total resisting moment, which can be expressed as:

[9] $$F_s \times H_s = \sum_{i=1}^{n} P_i \, h_i$$

where, P_i is the maximum tensile force in the reinforcement, h_i is the height to i^{th} reinforcement from the base of the wall and n is the number of reinforcements. F_s is the total horizontal driving force and H_s is height to the resultant horizontal driving force measured from the base of the wall (see Fig. 2). For a given displacement of the unstable soil mass, the tensile force developed in each reinforcement layer is obtained from the SRI Local model.

Once the moments are in equilibrium, R_T is the difference between horizontal driving forces and total resistance provided by the reinforcements. Besides the force equilibrium, above analytical framework ensures the displacement compatibility.

Successful implementation of the SRI Global model requires, proper application of boundary conditions encountered in a MSE wall. As schematically shown in Fig. 2, any reinforcement encountered in a MSE wall should fall into one of the following four categories:

(i) No impact from boundary conditions (Case 1): Mobilized length measured from the failure surface is less than the distance to the wall facing or to the free end. The equations derived from the SRI Local model are applicable without any modifications. This is the most common condition encountered in walls with extensible reinforcements using the minimum reinforcement length recommended in design guidelines.

(ii) Free end of the reinforcement is mobilized (Case 2): In this case, the maximum tensile force is obtained using the SRI Local model with $l = L_2$ (< L_1). As shown in Fig. 2, L_2 is the distance from the failure surface to the free end and L_1 is the distance from the failure surface to the wall facing. Additional increase in displacement will not result in further increase in reinforcement load. In walls with inextensible reinforcements, this boundary condition is often observed in the upper layers.

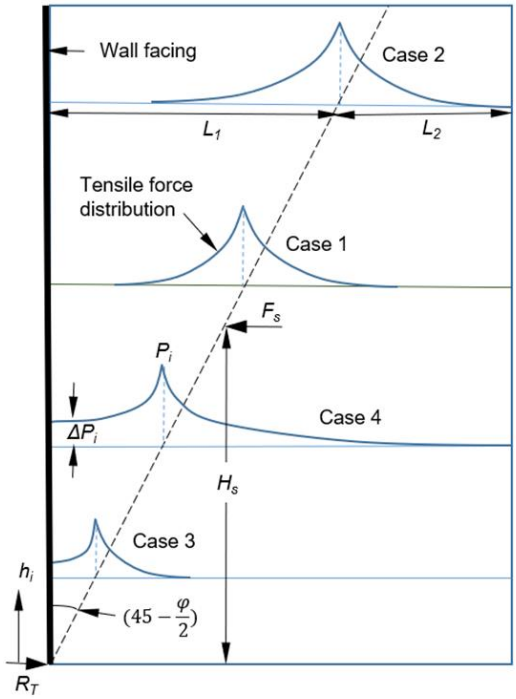

Fig. 2. Different boundary conditions experienced by reinforcements.

(iii) Resistance from the wall facing is mobilized (Case 3): The force in the reinforcement can be estimated using the SRI Local model until the mobilized length is equal to L_1 (< L_2). Beyond this displacement, any increase in displacement (Δu) will result in a net increase in tensile force (ΔP) which is given by the following:

[10] $$\Delta P = J_r \left[\frac{\Delta u}{L_1}\right]$$

The total tensile force along L_1 length is the summation of ΔP and the reinforcement load estimated from the SRI Local model using Eq. (8). Note that ΔP is the connection load developed at the facing. This is a common occurrence in bottom layers of walls reinforced with inextensible reinforcements.

(iv) Resistance of the wall facing and free length are mobilized (Case 4): Initially, the wall facing resistance is mobilized similar to Case 3. Further increase in displacement will mobilize L_2 length. When this occurs, tensile force will not increase further similar to Case 2. Unless the wall includes a truncated base, this is judged to be a rare occurrence and likely to occur in bottom reinforcements of walls with inextensible reinforcements.

The SRI model can be implemented in a spreadsheet as outlined by Weerasekara et al. (2017). Except for *Q* and *R* parameters in Bolton's equation, the input parameters used in the SRI model are not empirical and they can be obtained experimentally or through direct measurements. For geogrids, ribbed steel strips and steel wire meshes, pullout tests can be used to back calculate the interface friction which is otherwise difficult to determine directly. Once the input parameters are known, the solution can be obtained by gradually increasing the wall displacement until the resistance and demand moments are equal. Using nine full-scale instrumented walls reinforced with smooth and rough steel strips, Weerasekara (2018a) demonstrated that SRI method can successfully estimate the maximum reinforcement load distributions under working stress conditions. Although this approach is adopted by other researchers to validate the MSE design approaches, Weerasekara (2018a) highlighted the shortcomings of this approach of validating design methods where the methods are validated only under working stress conditions. Further details related to this aspect are discussed in subsequent sections.

Shortcomings of Existing Design Methods

Issue 1: Pullout Resistance Calculation

Pullout failure of reinforcement is recognized as one of the three failure modes associated with MSE walls although it is the rarest failure mode observed in practice (Bathurst et al., 2012, Holtz, 2017). While there are number of studies conducted to improve the predictions of P_{max}, there are only a limited number of methods to estimate the mobilized reinforcement length. The most recognized is the method outlined in the FHWA manual FHWA-RD-89-043 (Christopher et al. 1990) which is widely adopted in practice. According to this method, the mobilized reinforcement length (*l*) beyond the potential failure surface is estimated using the following empirical relationship:

$$l = \frac{P_{max}}{F^* \alpha \sigma_v C R_c} \quad [11]$$

where *C* is a factor that accounts for the reinforcement surface area, R_c is the reinforcement coverage ratio, α is a scale effect correction factor and F^* is the pullout resistance factor. The calculated length is further increased by applying an appropriate factor of safety for allowable stress design (or a resistance factor for the limit state design). The reinforcement stiffness, which is the most influential parameter for pullout response, is not explicitly considered and its impact is assumed to be captured indirectly in the empirical parameter α. Although method such as Simplified Stiffness method were developed to estimate the impact of reinforcement stiffness on P_{max}, once P_{max} is estimated, the pullout resistance is still estimated using Eq. (11) which fails to recognize the direct impact of reinforcement stiffness on the mobilized reinforcement length.

Recognizing the importance of α and F^* on the overall pullout resistance, it is critical to know how these parameters are determined. Current design guidelines recommend α and F^* be determined from direct shear and pullout tests. In a pullout test, reinforcement will continue to elongate before mobilizing the entire reinforcement length. Once the friction is fully mobilized over the entire reinforcement length, the trailing end will begin to move. For extensible reinforcements, Christopher et al. (1990) recommended α be determined at a deflection of 15 mm (5/8-inch) measured at the back of the reinforcement if the reinforcement does not rupture at this displacement. A minimum reinforcement embedded length of 600 mm is recommended for the pullout test. For inextensible reinforcements, corresponding α value is determined when the pulling end or trailing end displacement is 15 mm. Although above deflection limit was selected to limit the deformations in the walls, it is unclear how this unique displacement and reinforcement embedment length relate to the pullout occurrence or serviceability of the actual wall.

Eq. (11) assumes a linear relationship between pullout capacity and normal stress. However, numerous experimental studies have demonstrated that relationship between pullout capacity and overburden stress is nonlinear (e.g., Juran et al. 1998). This is attributed to constrained dilation of dense granular soils which diminishes as the soil overburden is increased. Even if experimental results are available for a certain overburden stress, that cannot be interpolated or extrapolated to other overburden stresses to estimate corresponding α and F^* values due to the empirical nature. It is not practical to conduct pullout tests at all potential overburden stresses to determine α and F^* values for

each reinforcement layer. Moreover, compared to the relationships developed for the SRI method, it is optimistic to assume that α and F^* parameters alone can capture the impact of reinforcement stiffness, overburden stresses and interface friction. Huang et al. (2010) study of the FHWA pullout model indicated a very poor accuracy for geogrids. To overcome the shortcoming, they proposed nonlinear and bi-linear relationships for α and F^* parameters that vary with the normal stress. Even this proposed modification does not consider the actual geogrid-soil interaction; therefore, key parameters such as reinforcement stiffness is absent in the formulation.

In contrast, Eq. (7) of the SRI model incorporates an improved interface friction model (i.e., SRI Friction model) and account for the soil-reinforcement interaction by incorporating the reinforcement stiffness (i.e., SRI Local model) and relevant boundary conditions and impact from other reinforcement layers in the wall towards equilibrium (i.e., SRI Global model). Weerasekara et al. (2017) and Weerasekara et al. (2010) demonstrated that pullout characteristics can be reliably determined using the SRI Local model by modelling large number of pullout tests. A true validation exercise should consider multiple pullout tests conducted at different reinforcement lengths, overburden stresses, etc. Initially, one test may be used to determine parameters such as the interface friction angle if direct measurements are not feasible. The remaining tests should be modelled by changing only the appropriate test variables to check if that will provide an accurate prediction of the measured pullout response. Furthermore, the validation exercise should not focus only on the pullout force - displacement relationship but should also consider interrelationships between displacement, strain and mobilized length since they are all related. For example, it may be possible to achieve a reasonable match for the pullout resistance versus displacement relationship while the prediction for the mobilized reinforcement length is poor. Although it is difficult measure the mobilized length directly, it is possible to measure the instance when the trailing end of the reinforcement starts to move. When this occurs, the mobilized reinforcement length is equal to the reinforcement length inside the pullout box. In pullout tests, this can be used to validate the predictions for the mobilized length.

Issue 2: Demand at Facing Connection

Besides the pullout and tensile rupture of the reinforcement, the tensile rupture of the reinforcement at the facing connection is recognized as a failure mode associated with MSE wall. As discussed in the subsequent section, this failure mode is more likely to occur in walls reinforced with inextensible reinforcements. Although the actual tensile demand is less than P_{max} at the facing connection, the tensile capacity of the reinforcement at the facing is generally small due to the allowances made for the connection. Therefore, it is critical to know the load transferred to facing connection to determine if the tensile capacity of the connection will be exceeded. However, none of the current design methods can estimate the load at the facing connection because of their inability to predict the load distribution along reinforcements. Therefore, it is typical to assume that tensile demand at the facing connection is equal to P_{max} which occurs elsewhere. This cannot be justified using known physics and also contradicts the observations from instrumented walls. The tensile load transferred to the facing connection is expected to be smaller than P_{max}, and will depend on J_r, P_{max} and L_1.

However in past experiments, it was observed that settlement of the soil behind the wall facing can create drag loads that are transferred to the reinforcement (Damians et al. 2015), especially near the top of the wall. Although the SRI method cannot estimate the these drag loads, they are unlikely to impact the global stability of the wall.

Issue 3: Ultimate Load, Failure Mode and Factor of Safety Calculations

Though existing design methods can predict the maximum reinforcement loads under working stress conditions with reasonable accuracy, they are not validated against the ultimate collapse limit state. The ability to predict the performance at working stress conditions is only part of the design challenge. Without validating their ability to predict the ultimate load carrying capacity, there is no guarantee that the estimated factor of safety or capacity/demand ratio under limit state design is accurate.

In the current practice, calculations are performed at each reinforcement layer and the failure of the entire reinforcement mass is assumed when the demand in at least one reinforcement exceeds the capacity of a select failure mode. Limitation of this assumption should be apparent especially when displacement-controlled failure modes such as reinforcement pullout are considered. For example, if the friction is fully mobilized in one or more reinforcement (i.e., factor of safety against pullout is unity), can that lead to the failure of the entire reinforced soil mass? The failure surface typically intersects several reinforcement layers. If the pullout resistance is fully mobilized in a certain reinforcement layer(s), further deformation of the wall can increase the contribution from the remaining reinforcement layers until equilibrium is attained. Above limitation may not cause a significant error in walls reinforced with extensible reinforcements

because the failure often occurs due to tensile rupture of the reinforcement away from the connection, and at that moment, the remaining reinforcements may not have a reserve capacity to accommodate the lost resistance from the ruptured reinforcement.

The best example to demonstrate the above limitation is the full-scale instrumented walls completed at the Waterways Experimental Station (WES). The test details and results are given in Al-Hussaini and Perry (1978). One wall was reinforced with smooth steel strips and other was reinforced with nylon strips. Apart from reinforcement type and horizontal reinforcement spacing, two walls were identical with respect to their final design height, vertical reinforcement spacing, reinforcement length, soil type and compaction effort. The walls were 4.9 m long, 3.1 m wide, designed to reach a height of 3.66 m. The steel strip wall was reinforced with six layers of smooth galvanized steel strips of 0.635 mm thick, 102 mm wide and 3.1 m long with a horizontal and vertical spacing of 0.77 m and 0.6 m, respectively. The steel strips were connected to the aluminium facings using double angle connectors and two 6.35 mm diameter bolts. The nylon strip reinforced wall included heavy neoprene-coated nylon fabric strips of 100 mm wide, 2 mm thick and 3.05 m long. While the vertical spacing was similar to the steel strip wall, the horizontal spacing of nylon strips was 1.2 m. Both walls were backfilled with clean sub-angular to angular concrete sand and nominally compacted. Details related to modelling of these two walls using the SRI method can be found in Weerasekara et al. (2017) and Weerasekara (2018b).

Using the current methods, both walls are predicted to fail due to pullout of the upper reinforcements. Although the nylon strip reinforced wall collapsed due to pullout while it was under construction, the steel strip wall experienced less than 5 mm of movement once it reached its design height. As the wall showed no signs of failure, it was surcharged to failure in increments of 12 kPa. Eventually, the wall collapsed when the loading when the surcharge was approximately 90.4 kPa. The inspections of the collapsed wall revealed failures at the facing connection. To the best of author's knowledge, the steel strip reinforced wall is the only wall in the public domain that can be used to validate the ultimate load carrying capacity of a wall reinforced with inextensible reinforcements; therefore, the observations cannot be ignored.

The performance of the wall under all stages of loading was modelled using the SRI model. For each loading increment, wall deformation was incrementally increased until the driving moment is equal to the resisting moment. Figs. 3(a) and (b) show the resisting and driving moments calculated prior to surcharging and with a surcharge of 90 kPa. According to the SRI method predictions, at a surcharge of 90 kPa, the failure was imminent as the connection load in the bottom three layers have approached the tensile strength limit. When this threshold load is exceeded, tensile rupture was simulated by setting the connection strength to zero. This is reflected in the sudden reduction in the resisting moment in Fig. 3(b). According to the SRI method predictions, failure was initiated by the tensile rupture of one of the strips in the bottom three layers at the facing connection. The failure would have been sudden and brittle as the remaining layers are not able to accommodate the surplus load, which is consistent with the actual failure observations. To estimate the failure of this wall, the design method should be able to estimate the distribution of the reinforcement load along the reinforcement, including the force transmitted to the facing connection. Except for the SRI method, other design approaches cannot estimate the load transmitted to the facing connection and there are serious deficiencies in the pullout estimations as highlighted above.

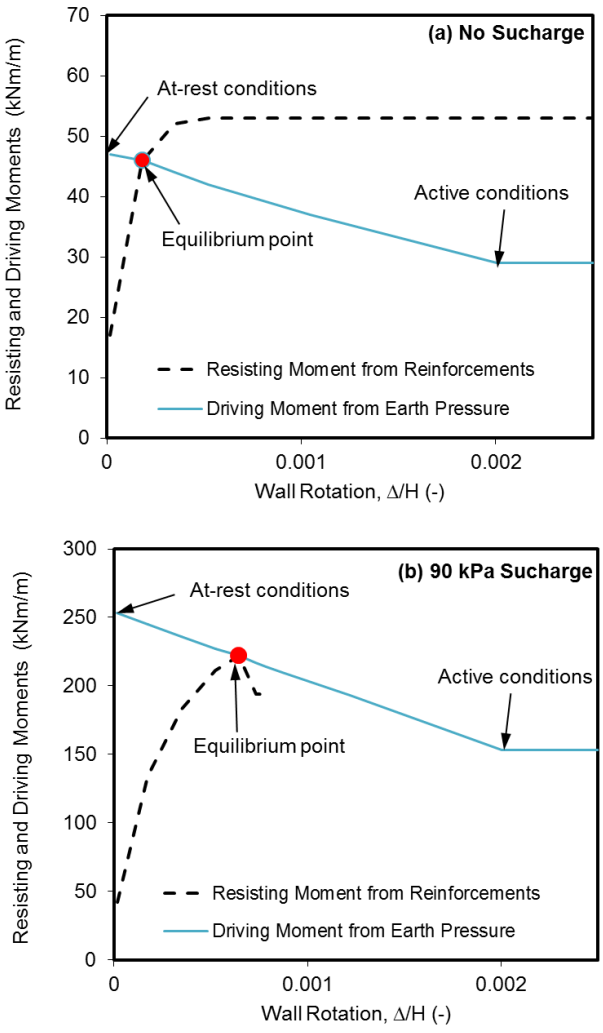

Fig. 3. Resisting and driving moments calculated (a) prior to surcharging and (b) with a surcharge of 90 kPa for steel strip reinforced WES wall.

In walls with inextensible reinforcements, another limitation of the pullout resistance calculation using the existing approaches is evident when examining the load (or strain) distributions along reinforcements in instrumented walls. With a minimum factor of safety of 1.5 targeted against pullout under working stress conditions, tensile force is expected to reach zero well before the end of the reinforcement. In other words, Case 2 and 4 boundary conditions should not prevail under working stress conditions according to the existing design methods. However, this contradicts the actual reinforcement strain distributions observed in instrumented walls with inextensible reinforcements, especially near the top of the wall. For example, Runser et al. (2001) published the reinforcement load distributions of the 16.9 m high Minnow Creek wall that was reinforced with ribbed steel strips. The reinforcement length was 15.4 m in the bottom four layers and 12 m in the remaining layers (Fig. 4). The reinforcement load distributions obtained under working stress conditions indicated full mobilization of friction in reinforcement layers located approximately in the upper 12 m (Fig. 5). Each reinforcement layer would have been designed with a minimum factor of safety of 1.5 against pullout. However, the measured reinforcement strain distributions contradict this assertion as the actual factor of safety against pullout is unity in the upper reinforcements even under working stress conditions. As indicated by the small wall deformations measured after construction (i.e., only 30 mm for the 16.9 m high wall), the wall is not at risk of failure from pullout and likely to have satisfied the design intent.

Even in the WES steel strip wall, the existing design approaches would estimate a factor of safety less than unity against pullout in the upper reinforcement layers prior to surcharging of the steel strip reinforced wall. For the WES steel strip wall, it is interesting that the SRI method also predicts full mobilization of reinforcement length in the upper four reinforcement layers (i.e., factor of safety of one) which is consistent with the actual field measurements. The maximum tensile force developed in the upper reinforcement layers were governed by Case 2 boundary condition, such that further increase in wall displacement would not increase the tensile demand as the entire reinforcement length is already mobilized. This is expected as steel strips require only a small displacement to mobilize its entire reinforcement length due to its relatively high stiffness.

Question remains why these two walls did not fail even when most of the reinforcement layers mobilized their maximum pullout resistance? The SRI method shows that only a small fraction of soil strength is mobilized when the equilibrium is reached under working stress conditions although most of the reinforcement contribution is utilized. This is apparent when comparing the demand/resistance plots. The safety margin is largely provided by the soil resistance that has not been mobilized. Above is consistent with the following statement made by Prof. Bob Holtz during the 2017 Terzaghi lecture: "*With steel-reinforced soil, the steel does most of the work, and the sand just goes along for the ride. Not so with geosynthetic reinforcement*". Although this has been common knowledge, only SRI method can provide an analytical explanation to verify this assertion.

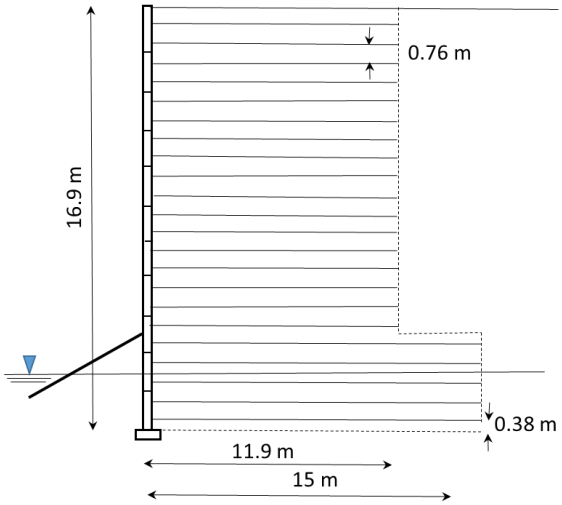

Fig. 4. Wall geometry of Minnow Creek Wall

Furthermore, analysis of the WES steel strip wall demonstrates that failure was governed by more than one failure mode (i.e., pullout of the upper reinforcements and tensile failure of the bottom reinforcements at the facing connection). Sensitivity analyses carried out by the author on other steel strip reinforced walls have indicated a similar failure mechanism in walls built to current standards. This complex interaction between different reinforcements and gradual mobilization of soil and reinforcement resistances could not be demonstrated using other design methods.

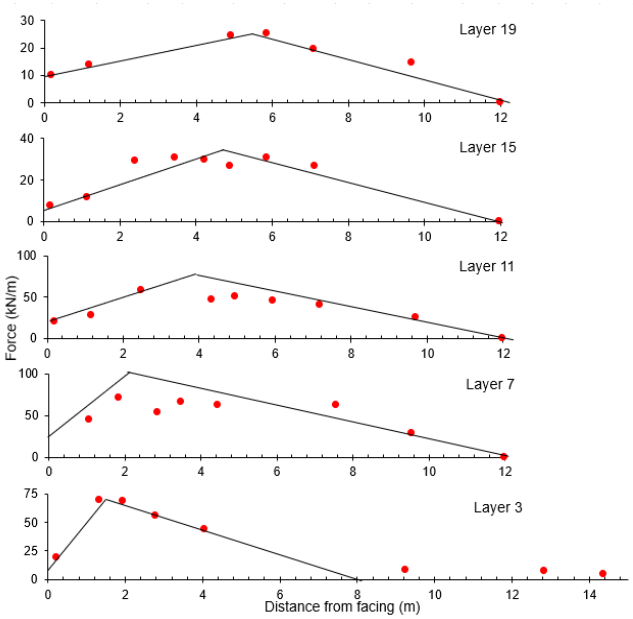

Fig. 5. Measured reinforcement load distributions in Minnow Creek Wall (reproduced from Runser et al. 2001).

The WES nylon strip reinforced wall is a rare occurrence where the wall failure can be attributed to pullout. The failure of the wall occurred due to pullout after reaching a wall height of 3.05 m. Fig. 6 shows the resistance and demand curves obtained using the SRI method. Compared to the steel strip wall, relatively low reinforcement stiffness leads to a slow development of resistance compared to the sharp increase in resistance observed in the steel strip reinforced wall. As a result, the nylon strip wall requires a larger displacement to reach equilibrium, which is greater than the displacement required to mobilize the active soil resistance. This constitutes to the pullout failure of the reinforced soil mass.

Two WES walls demonstrate the importance of reinforcement stiffness and its influence on the failure mechanism. For example, in the absence reinforcement stiffness in the formulation, the existing methods would predict pullout failures in both walls. In contrast, the SRI method correctly predicted the failure of the nylon strip reinforced wall; more importantly, the non-failure of the steel strip reinforced wall prior to surcharging. Besides explaining the failure modes, these demand/resistance plots can also explain the ductile or brittle behaviours observed in structures reinforced with different reinforcement types.

.

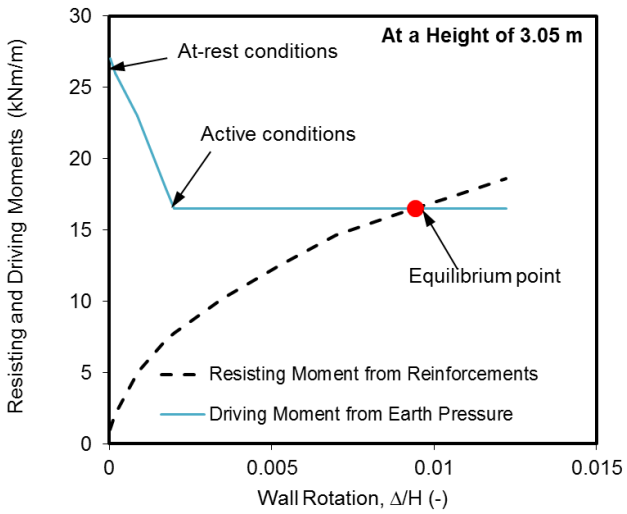

Fig. 6. Resisting and driving moments calculated for the nylon strip reinforced WES wall at height of 3.05 m.

Despite the differences in reinforcement types, the SRI method demonstrates that fundamental wall behaviours are similar in these two walls if the soil-reinforcement interaction is considered. This is a vital observation since SRI method does not require to assign different design parameters (e.g., lateral earth pressure coefficients) or adopt a different design method for these two walls as recommended in existing design codes and standards. Instead, using the correct reinforcement stiffness and interface friction angle, the behaviours of MSE walls with different reinforcement types can be explained

The SRI method shall not be considered as a working stress nor as a limit equilibrium-based method. For example, it is not required for all reinforcements and soil to reach their limit state at once as required in limit equilibrium-based method which is not a realistic assumption especially in walls with inextensible reinforcements. As evident in the WES steel strip reinforced wall, certain reinforcements can reach their maximum capacity even under working stress conditions. As the loading is increased, additional resistance is provided by the remaining reinforcements and soil. The SRI method can estimate the reinforcement loads under all stages of loading ranging from working stress conditions to ultimate state.

Issue 4: Unique Wall Configurations and Ability to Optimize

The empirical methods can only be applied if the wall in question falls within the database that was used to calibrate the model. With walls designed to greater heights and different reinforcement configurations, the applicability of empirical methods is constrained. In comparison, under working stress conditions, Weerasekara et al. (2018a) demonstrated that SRI method can estimate the maximum reinforcement

load in steel strip reinforced walls using known theories without relying on empirical parameters calibrated from instrumented walls. Unlike empirical methods, each input parameter used in the SRI model can be verified by using independent tests.

Solely from an internal stability standpoint, the SRI method shows the potential for using different reinforcement lengths and strengths for improving the overall factor of safety or optimize the design, as opposed to using uniform reinforcement lengths irrespective of the actual design needs. For example, in the case of WES steel strip wall, the overall load carrying capacity of the wall can be increased by (a) using longer reinforcements in the upper layers and (b) strengthening the facing connections or reduce the demand in the bottom layers by decreasing the spacing between reinforcements. This example further demonstrates that shorter reinforcement lengths can be utilized in the bottom reinforcements as the mobilized length is less than the upper reinforcements. It is unfortunate if limitations in the database prevents implementation of measures to increase the robustness and reduce the construction cost.

In certain situations, accommodating uniform reinforcement lengths can become an expensive design proposition if competent soil or bedrock is to be excavated and removed to accommodate the reinforcement length. If the external stability requirements are satisfied, there is no basis to undertake such excavations such that the newly designed wall falls into the database used for the calibration of the design method. FHWA (Berg et al (2009) allows shortening of the bottom reinforcements to minimize excavation requirements if the wall is founded on rock or competent foundation soil. In such situations, for analysis purposes, FHWA recommends dividing the wall into rectangular sections of uniform lengths. It is unclear if such conditions can be accommodated by the empirical design method since the wall configuration may fall outside the database used for calibration of the method. Furthermore, for each wall section, pullout calculations are performed for each reinforcement layer; thus, the same limitations discussed in the preceding sections will prevail. Comparatively, the SRI method provides a rational basis to accommodate truncated reinforcements at the base after considering realistic failure modes for the entire soil mass.

Likewise, when the reinforcement length is limited by vertical or horizontal obstructions (e.g., manholes, utilities, culverts), the SRI method provide a framework to estimate the impact of the shorter reinforcement length. As the overall factor of safety is not necessarily depends on the weakest reinforcement, reduced contribution from a shorter reinforcement can be compensated by making changes to the remaining layers (i.e., using stiffer and/or longer reinforcements). FHWA (Berg et al (2009) also recommends the surrounding reinforcement layers be designed to carry the additional load which would have been carried by the shortened reinforcement(s). However, there are concerns related to the implementation of this recommendation as the existing design methods fail to consider a realistic failure mechanism and overall factor of safety is still governed by the weakest layer. In addition, when attempting to compensate for vertical and horizontal obstructions, effectiveness of closely spaced reinforcements is questionable when using tributary area based methods - see further discussions in the next section.

Issue 5: Tributary Area Based Framework

While SRI method does not follow the tributary area concept, other design methods calculates P_{max} as the product of the contributory area and average horizontal stress acting on that area. It should be reminded that this tributary area concept is only a simplification for the complex soil-reinforcement interaction occurring in MSE walls. The shortcoming of the tributary area method may not be readily apparent in walls with equally spaced reinforcements. The difference between tributary area methods and SRI method can be demonstrated using the following hypothetical example. The wall shown in Fig. 7a has three layers of continuous reinforcements with uniformly distributed layers. For an assumed horizontal earth pressure distribution, the tributary area method will estimate the smallest and largest tensile loads in reinforcement layers A and C, respectively. For comparison, a wall with closely spaced reinforcements can be considered as shown in Fig. 7b. The separation between reinforcements can be nominal such that frictional resistance of each reinforcement is not impacted by the neighbouring reinforcements. If the wall is in equilibrium, tributary area methods will estimate a very small tensile load in reinforcement layer B due to the small tributary area, while relatively large reinforcement loads are estimated for reinforcement layers A and C. In comparison, the SRI method will estimate similar tensile forces in all three reinforcement layers as they experience approximately similar vertical overburden stress (i.e., friction forces) and elongation to achieve displacement compatibility. It can be argued that SRI model predictions are more realistic although there are no numerical modelling or test walls constructed to verify the load distributions when reinforcements are spaced close to each other.

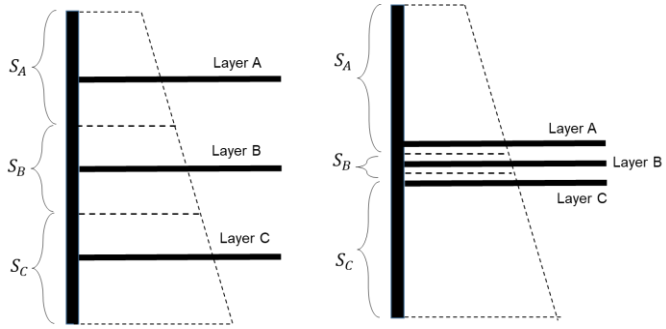

Fig. 7. Tributary areas for two hypothetical wall configurations (a) uniformly and (b) closely spaced reinforcements.

Issue 6: Impact of Wall Toe Resistance

Several studies have highlighted the importance and influence of toe resistance on the magnitude and distribution of reinforcement loads (Huang et al. 2010; Leshchinsky and Vahedifard, 2012; Ehrlich and Mirmoradi, 2013). The reduced reinforcement load near the wall base can be attributed to the toe resistance generated from the soil embedment and friction. The toe resistance is not explicitly mentioned in existing design methods although it can be argued that it is implicitly considered since the design methods were developed from measurements obtained from actual instrumented walls where the toe resistance would have impacted the measurement. However, the toe resistance built into these empirical methods cannot be quantified. As a result, it is not possible to determine whether such magnitude of toe resistance would exist in a newly designed wall or allow the designer to adjust the toe resistance depending on the site conditions. In contrast, the SRI model allows the toe resistance to be quantified and adjusted if required.

According to the database compiled by Allen and Bathurst (2003), the normalized P_{max} distribution in walls with extensible reinforcements is trapezoidal with reinforcements near the bottom experiencing very small tensile load. Comparatively, in walls with inextensible reinforcements, much larger contribution is provided by the bottom reinforcements resulting in a more triangular shaped normalized P_{max} distribution. With inextensible reinforcements, the wall will reach its force equilibrium at a much smaller displacement/rotation. Therefore, a smaller soil resistance is mobilized at the toe of the wall; hence, a significant reduction in tensile load is not expected compared to reinforcements in the upper layers. This behavior is analytically explained using the SRI method.

Issue 7: Extensibility of Reinforcement and Uniqueness of P_{max} Distribution

The current design methods require the lateral earth pressure distribution to be pre-determined based on the extensibility of the reinforcement. For this purpose, reinforcements are classified either as extensible or inextensible based on the material type regardless of the actual elongation experienced by the reinforcement. Even if the same reinforcement is used in every layer, as evident in instrumented walls, reinforcements at different depths will experience different reinforcement strains such that extensible and inextensible conditions can coexist in the same wall. For example, this is evident in the database compiled by Allen and Bathurst (2003) where small strains have been measured in the bottom and upper reinforcement layers even when the wall is reinforced with extensible reinforcements. A polymer reinforcement located at a shallow depth may not experience a large elongation because the interface friction is not sufficient to develop large strains in the reinforcement. Likewise, an extensible reinforcement placed at the bottom of the wall may not develop significant strain as it is not required to elongate significantly if the wall is rotating about its base. Although some attempts have made to classify reinforcement extensibility by comparing against the soil stiffness, preceding sections indicate the limitations of using such approaches as the extensibility depends on many other factors. For example, British Standards (BS8006) recommends using the Tie-back Wedge method for walls with reinforcement strains exceeding than 1% and Coherent Gravity method for strains below this limit. It is unclear how a unique value of 1% is selected as the threshold for deciding significantly different lateral earth pressure distributions and design methods. For certain polymeric reinforcements with high strength and stiffness, it is uncertain if the reinforcement should be treated as extensible or inextensible. For example, Miyata et al. (2018) had to conduct a separate study to confirm that polyester straps should be considered as an extensible reinforcement in the Simplified Stiffness method.

In contrast, the SRI method does not require the reinforcement extensibility to be predetermined to decide the lateral earth pressure distribution. Most importantly, the SRI method shows that behaviors of extensible and inextensible reinforcements are fundamentally similar. It is not required to adopt different design parameters or lateral earth pressure distributions if the soil-reinforcement interaction is properly accounted. If required, normalized P_{max} distributions can be obtained from the SRI method as an output. As indicated in Weerasekara et al. (2017), the results are consistent with different shapes of P_{max} distributions observed in full-scale instrumented walls with extensible and inextensible reinforcements.

Furthermore, the SRI method shows that the normalized P_{max} distribution measured under working

stress conditions will not remain the same at all stages of loading, including the ultimate state. For example, using the results of an instrumented wall completed at the Royal Military College of Canada (RMCC), Weerasekara et al. (2017), demonstrated that the normalized reinforcement load distribution obtained before surcharging is approximately similar to the trapezoidal load distribution considered in the original version of the K-Stiffness method where the reinforcement loads are small at the top and bottom (see Fig. 8). However, as the surcharge is increased up to failure, the relative contribution from the upper reinforcements have increased considerably causing the shape of the P_{max} to change. In comparison, in the WES steel strip wall, the normalized P_{max} distribution is changed slightly from its original shape as the wall is surcharged. These behavioral differences can be explained using the SRI method by considering the soil-reinforcement interaction and boundary conditions.

Issue 8: Contradictions with Known Theories

In certain instances, the existing design methods may appear to contradict known soil mechanic theories. The SRI method can demonstrate that such conclusions can arise due to erroneous interpretation of results using frameworks that fail to recognize the soil-reinforcement interaction. For example, for the development of the Coherent Gravity method, Baquelin (1978) suggested that the at-rest lateral earth pressure will prevail near the top of the wall which will decrease with depth until active earth pressure is reached at 6 m below the top of the wall. Although this interpretation is consistent with the back-calculated lateral earth pressure coefficients based on tributary area based methods, this contradicts other experimental and numerical investigations conducted on lateral earth pressures (e.g., Chang, 1997; Kezdi, 1958). Typically, the lateral earth pressure coefficient is expected to be smaller at the top compared to the bottom if the wall is rotating about its base as the largest deformations are expected at the top. This confusion can be explained using the SRI method, which can show that the back-calculated lateral earth pressure coefficient in the Coherent Gravity method is an outcome of the soil-reinforcement interaction and not a reflection of the actual lateral earth pressure coefficient; hence, there is no contradiction.

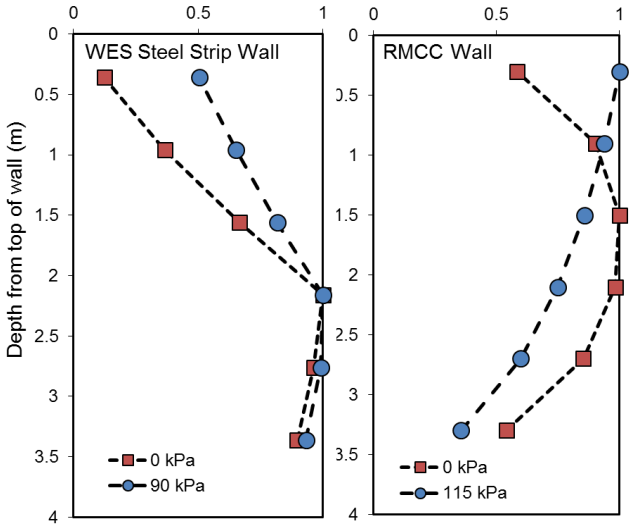

Fig. 8. Distributions of normalized maximum reinforcement loads with depth before surcharging and immediately before failure for (a) RMCC wall and (b) WES steel strip wall.

The SRI method can provide analytical explanations to some of the characteristics observed in instrumented walls. Besides simple observations such as the differences in displacements measured in walls with inextensible and extensible reinforcements, the SRI method can explain more complex behaviors such as the differences in normalized P_{max} distributions under working stress conditions when extensible and inextensible reinforcements are utilized. Furthermore, using the pullout tests conducted by Jayawickrama et al. (2013) on ribbed steel strips, Weerasekara et al. (2017), demonstrated how observed trends in F^* with depth can be explained using known soil mechanic theories (see Fig. 9). Test details and input parameters used in the prediction are summarized in Weerasekara et al. (2017); therefore, not repeated herein for brevity. Note that F^* parameter in the Coherent Gravity method is related to T_1 in the SRI Friction model especially when inextensible reinforcements are concerned.

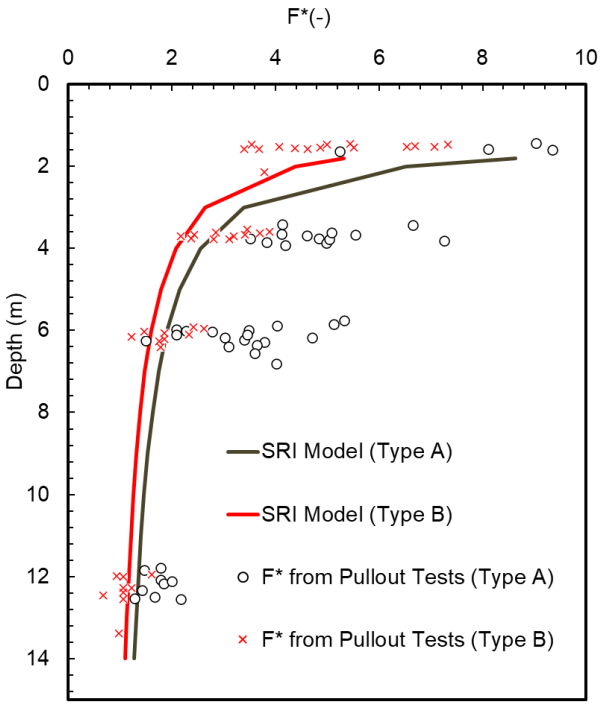

Fig. 9. *F** values estimated from the SRI Friction model and measured from pullout tests conducted on steel ribbed steel strips (adopted from Jayawickrama et al. 2013).

Summary

The SRI method relies on a vastly different analytical framework to assess the internal stability of MSE walls compared to the existing empirical design methods that depends on the tributary area concept. The paper highlighted several limitations of existing design methods and how those can be overcome using the SRI method, and they are summarized below:

- The greatest benefit of the SRI method is in the ability to estimate a more reliable factor of safety and ultimate load carrying capacity as opposed to assuming that the lowest factor of safety calculated for each reinforcement is equal to the factor of safety of the entire wall. The shortcoming of this assumption is more apparent in walls reinforced with inextensible reinforcements. The current design methods such as the Simplified Stiffness, Coherent Gravity and AASHTO Simplified methods have been validated only under working stress conditions. To demonstrate that a design method can achieve a reliable factor of safety (or capacity/demand ratio as per limit state design), it should also be capable of predicting the ultimate state accurately. Without a reliable method to estimate the mobilization of tensile force along the reinforcement and load transmitted to the facing connection, it is not possible to estimate the ultimate state. Although the SRI method can estimate the factor of safety of each reinforcement layer and for each of the three failure modes, those should not be relied upon to determine the factor of safety of the entire soil mass due to limitations explained in this paper.
- The paper explained key limitations in estimating the pullout resistance using the FHWA approach (Christopher et al. 1990) and assumption that load transmitted to the facing is similar to P_{max} that occurs elsewhere. Using of reinforcement stiffness in the soil-reinforcement interaction computation, the SRI method provides an improved framework to estimate the tensile load distribution and load transmitted to the facing connection.
- In inextensible reinforcements, often the tensile force is mobilized along the entire reinforcement length even under working stress conditions (i.e., factor of safety of unity), which does not reflect the minimum factor of safety targeted by the designer using the current design methods. However, the SRI method demonstrates that this condition alone is not sufficient to cause failure of the entire wall. Additional resistance is provided by the remaining reinforcement layers and soil. Surcharging may cause the bottom reinforcements to reach their tensile capacity at the facing connection. In such situations, the wall failure is caused by the combination of pullout of the upper reinforcements and tensile rupture of the bottom reinforcements at the facing connection. This complex failure mode cannot be simulated using the existing design methods.
- The SRI method facilitates design optimization by utilizing non-uniform reinforcement lengths and allowing walls with different heights and configurations be designed as the analysis method is not constrained by the database used for calibration. The method also provides a rational framework to design for vertical and horizontal obstructions and justify non-uniform reinforcement configurations in lieu of excavating and removing competent bedrock or soil to achieve a uniform reinforcement length.
- The SRI model allows the toe resistance to be quantified and allow the designer to adjust it to suit the field conditions. In comparison, toe resistance built into the existing design methods cannot be quantified or modified to match the site conditions.
- The SRI method does not require the reinforcement extensibility to be predetermined to decide the shape of P_{max} distribution with depth. In addition, it is incorrect to assume that P_{max} distribution will remain the same as the working stress conditions when the loading conditions change.

- The SRI method demonstrates that wall behaviors can be explained using known theories and conventional input parameters without resorting to an empirical approach. The known theories can be used to explain the observed behaviors without any contradictions.
- The SRI method demonstrates that behaviors of extensible and inextensible reinforcements are fundamentally similar if the soil-reinforcement interaction is properly accounted. As a result, the SRI method can explain different reinforcement load distributions, ductility/brittleness behaviors, observed failure modes, etc. In essence, there is no reason to use vastly different design methods and empirical design parameters depending on material used for reinforcing.

Similar to other soil-structure interaction problems, the SRI method can be implemented in the allowable stress design domain only. Any alteration to the input parameters using resistance factors could alter the failure mechanism. The input parameters should be as realistic as possible because it is not straightforward to determine if the select input parameter will result in a conservative design. It is appropriate to conduct parametric analysis to determine the robustness of the design.

One of the drawbacks of the SRI method is that the wall deformations estimated using this method are considerably smaller than those measured instrumented walls especially if extensible reinforcements are utilized. It is important to note that displacements estimated using the SRI model are associated with the strain in the reinforcements. Any slack in the reinforcement, deformations in the soil mass and bulging of the facing will result in additional deformations which cannot be accounted using the SRI method. Furthermore, the analytical formation in the SRI method cannot model the connection load that may develop from downward movement of backfill immediately behind the facing.

References

AASHTO. 2020. LRFD Bridge Design Specifications. 9th Edition, American Association of State Highway and Transportation Officials, Washington, D.C.

Al-Hussaini, M., and Perry, E. B. 1978. Field experiment of reinforced earth wall. Journal of Geotechnical Engineering Division, ASCE, 104(3): 307–322.

Allen, T. M., and Bathurst, R.J. 2015. Improved simplified method for predictions of loads in reinforced soil walls. Journal of Geotechnical and Geoenvironmental Engineering, 141(11): http://dx.doi.org/10.1061/(ASCE)GT.1943-5606.0001355.

Allen, T. M., and Bathurst, R.J. 2003. Predictions of reinforcement loads in reinforced soil walls. Revised Report No. WA-RD 522.2, Washington State Department of Transportation (WSDOT), Olympia, Washington.

Allen, T. M., Bathurst, R. J., Holtz, R. D., Lee, W. F., and Walters, D. L. 2004. A new working stress method for prediction of loads in steel reinforced soil walls. Journal of Geotechnical and Geoenvironmental Engineering, 130(11): 1109 – 1120.

ASTM. 2001. Standard test method for determining tensile properties of geogrids by the single or multi-rib tensile method. D6637, West Conshohocken, Pennsylvania.

Baquelin, F. 1978. Construction and Instrumentation of Reinforced Earth Walls in French Highway Administration. ASCE, Pittsburgh, pp. 186–201.

Bathurst, R.J, Huang, B., and Allen, T.M (2012). LRFD calibration of the ultimate pullout limit state for geogrid reinforced soil retaining walls. International Journal of Geomechanics. 12: 399-413. 10.1061/(ASCE)GM.1943-5622.0000219.

Berg, R.R. Christopher, B.R., Samtani, N.C. 2009. Design and construction of mechanically stabilized earth walls and reinforced soil slopes – Volume 1, Publication No. FHWA-NHI-10–024, U.S. Department of Transportation, Federal Highway Administration, Washington, D.C.

Bolton. M. D. 1986. The strength and dilatancy of sands. Geotechnique, 36(1): 65-78.

Canadian Standards Association. 2019. Canadian Highway Bridge Design Code (CHBDC). CSA Standard S6:19, Canadian Standards Association, Toronto, Canada.

Chang, M-F. 1997. Lateral earth pressure behind rotating walls, Canadian Geotechnical Journal, 34: 498-509.

Christopher, B. R., Gill, S. A., Giroud, J.-P., Juran, I., Mitchell, J. K., Schlosser, F., and Dunnicliff, J. 1990. Reinforced soil structures, Volume 1: Design and Construction Guidelines. Federal Highway Administration (FHWA), Report No. FHWA-RD-89-043, Washington, D.C.

Damians, P., Bathurst., R.J, Josa, A., and Lloret, A. (2015). Numerical analysis of an instrumented steel reinforced soil wall, ASCE International journal of Geomechanics, 15(1): p. 04014037.

Ehrlich, M., and Mirmoradi, S. H. 2013. Evaluation of the effects of facing stiffness and toe resistance on the behavior of GRS walls. Geotextiles and Geomembranes, 40(1): 28 – 36.

Holtz, R. (2017). 46th Terzaghi Lecture: Geosynthetic reinforced soil: From the experimental to the familiar. Journal of Geotechnical and Geoenvironmental Engineering. 143. 10.1061/(ASCE)GT.1943-5606.0001674.

Huang, B., Bathurst, R. J. Hatami, K., and Allen, T. M. 2010. Influence of toe restraint on reinforced soil segmental walls. Canadian Geotechnical Journal, 47(8): 885 – 904.

Huang, B and Bathurst, R. J. (2009). Evaluation of soil-geogrid pullout models using a statistical approach. Geotechnical Testing Journal, 32. 10.1520/GTJ102460.

Jayawickrama, P., Surles, J.G., Wood, T.D., Lawson, W.D. 2013. Pullout resistance of mechanically stabilized reinforcement in backfills typically used in Texas. Research Report No. FHWA/TX-13/0-6493-R1, Vol. 1, Texas DOT, Austin, Texas.

Juran, I., Guermazi, A., Chen, C.L. and Ider, M.H. (1988). Modelling and simulation of load transfer in reinforced soil: Part 1, International Journal of Numerical Analytical Methods in Geomechanics, Vol.12, pp. 141-155.

Kezdi, A. 1958. Earth pressure on retaining wall tilting about the toe. Proceedings of the Brussels Conference on Earth Pressure Problems, Vol. 1, pp. 116–132

Leshchinsky, D., and Vahedifard, F. 2012. Impact of toe resistance in reinforced masonry block walls: Design dilemma. Journal of Geotechnical and Geoenvironmental Engineering, 138(2): 236-240.

Miyata, Y., Bathurst, R.J., and Allen, T.M. 2018. Evaluation of tensile load model accuracy for PET strap MSE walls, Geosynthetic International, 25(6): 656-671.

Runser, D. J., Fox, P. J., and Bourdeau, P. L. 2001. Field performance of a 17 m-high reinforced soil retaining wall, Geosynthetic International, 8(5): 367–391.

Schlosser, F. 1978. History, current development, and future developments of reinforced earth. Symposium on Soil Reinforcing and Stabilizing Techniques, Sydney, pp. 5–28.

Weerasekara, L. 2018a. Steel strip reinforced soil walls at working stress conditions, In proceeding of 71st Canadian Geotechnical Conference, GeoEdmonton, Edmonton, Canada.

Weerasekara, L. 2018b. Improvements to pullout failure estimation in MSE walls, In proceeding of 71st Canadian Geotechnical Conference, GeoEdmonton, Edmonton, Canada.

Weerasekara, L., and Wijewickreme, D. 2010. An analytical method to predict the pullout response of geotextiles. Geosynthetic International, 17(4): 193-206.

Weerasekara, L., Hall, B.E., and Wijewickreme. 2017. A New Approach for Estimating Internal Stability of Reinforced Soil Structures, Geosynthetic International, 24(4): 419 – 434.